**PAPER** • **OPEN ACCESS**

# Collective excitation of spatio-spectrally distinct quantum dots enabled by chirped pulses

To cite this article: Florian Kappe *et al* 2023 *Mater. Quantum. Technol.* **3** 025006

IOP Publishing Mater. Quantum Technol. 3 (2023) 025006 https://doi.org/10.1088/2633-4356/acd7c1

Materials for Quantum Technology



OPEN ACCESS

RECEIVED
9 March 2023

REVISED
2 May 2023

ACCEPTED FOR PUBLICATION
22 May 2023

PUBLISHED
2 June 2023



PAPER

# Collective excitation of spatio-spectrally distinct quantum dots enabled by chirped pulses

**Florian Kappe[1,6], Yusuf Karli[1,6], Thomas K Bracht[2,5], Saimon Filipe Covre da Silva[3], Tim Seidelmann[4], Vollrath Martin Axt[4], Armando Rastelli[3], Gregor Weihs[1], Doris E Reiter[2] and Vikas Remesh[1,*]**

[1] Institut für Experimentalphysik, Universität Innsbruck, Innsbruck 6020, Austria
[2] Condensed Matter Theory, Department of Physics, TU Dortmund, Dortmund 44221, Germany
[3] Institute of Semiconductor and Solid State Physics, Johannes Kepler University Linz, Linz 4040, Austria
[4] Theoretische Physik III, Universität Bayreuth, Bayreuth 95440, Germany
[5] Institut für Festkörpertheorie, Universität Münster, Münster 48149, Germany
[6] These two authors contributed equally.
[*] Author to whom any correspondence should be addressed.

**E-mail:** vikas.remesh@uibk.ac.at

**Keywords:** quantum dots, electron–phonon interaction, chirped pulses

Supplementary material for this article is available online

## Abstract

Nanoscale bright sources that produce high-purity single photons and high-fidelity entangled photon pairs are the building blocks to realize high security quantum communication devices. To achieve high communication rates, it is desirable to have an ensemble of quantum emitters that can be collectively excited, despite their spectral variability. In case of semiconductor quantum dots, Rabi rotations are the most popular method for resonant excitation. However, these cannot assure a universal, highly efficient excited state preparation, due to the sensitivity to excitation parameters. In contrast, adiabatic rapid passage (ARP), relying on chirped optical pulses, is immune to quantum dot spectral inhomogeneity. Here, we show that the robustness of ARP holds true for the simultaneous excitation of the biexciton states in multiple, spatially separated and spectrally different quantum dots. For positive chirps, we also find a regime where the influence of phonons relax the sensitivity to spectral detunings and lower the needed excitation power. Being able to generate high-purity photons from spatially multiplexed quantum dot sources using the biexciton to ground state cascade is a big step towards the implementation of high photon rate, entanglement-based quantum key distribution protocols.

## 1. Introduction

Semiconductor quantum dots are high-brightness and high-purity sources of single photons with low multiphoton rate [1–6] and high-fidelity entangled photon pairs [7–10] with near-deterministic operating nature [11]. In addition to these, the opportunity to engineer their properties optically [12–14], electrically [15, 16], or via strain-tuning [17–19] and growth processes [20] makes them the ideal platform to implement high-security quantum communication protocols, for instance quantum key distribution [21, 22]. Previous works on quantum key distribution with quantum dot sources [8, 23–27] targeted the optimization of brightness, entanglement fidelity and photon purity from single quantum dots. However, to ensure a high communication rate in protocols like BB84 [21], it is desirable to have an ensemble of quantum dots not only engineered to different wavelengths but also that can be collectively excited with high fidelity. To this end, the standard approach of resonant excitation [28–30] will only work for strictly-identical quantum dots, due to its sensitivity to the quantum dot properties and fluctuations in laser parameters. Therefore, in reality, a tailored resonant laser pulse (i.e. frequency and $\pi$ power) that fully inverts the population in one quantum dot will be dysfunctional [29, 31, 32] and even counterproductive in another as shown experimentally below.

One can employ multiple, independently-shaped laser pulses to address these variabilities, however this is a financially draining, resource-inefficient and space-consuming approach in addition to requiring synchronization of laser pulses to avoid timing errors in practical applications. In particular the number of required pulse-shapers in such schemes scales linearly with the number of quantum dots. Such independently-shaped pulses would then have to be site-specific to the target quantum dot, making the experiments extremely challenging. Notably, schemes like widefield excitation [33], structured illumination [34], and the recent dual-confocal [35] have been demonstrated for simultaneous excitation of an ensemble of emitters. However, such methods involve complex alignment processes and illumination engineering, in addition to requiring higher excitation powers.

Hence, an important question is how to develop a robust excitation scheme, i.e. one whose efficiency is insensitive against the spatio-spectral variability in the excitation conditions, that can coherently manipulate a quantum dot ensemble. One such scheme is based on chirped excitation via adiabatic rapid passage (ARP), which already has been demonstrated on single quantum dots [36–40]. For the production of single photons, ARP can work simultaneously on several quantum dots [41–43], where just the exciton was addressed.

In this paper, we demonstrate the simultaneous preparation of the biexciton states in a quantum dot ensemble via two-photon ARP without modifying the excitation parameters, i.e. using a single chirped laser pulse. Interestingly, we also find a regime of *phonon advantage*, where a positively chirped excitation and phonon-assisted state preparation interplay. This regime provides an extended spectral range for high efficiency excitation of biexciton states in multiple quantum dots at moderate pulse areas. This is different from a pure phonon-assisted excitation [44–50], which requires high pulse areas. We demonstrate a way to simultaneously address and populate multiple quantum dots with largely relaxed requirements on pulse frequency and power. Exciting the biexciton state is of particular interest since it can generate entangled photon pairs for various encoding schemes, e.g. polarization or time-bin [8, 51, 52], in addition to offering a simple method to generate multiplexed single photons, towards advanced quantum communication protocols. Our results pave the way for practical realization of spatio-spectrally multiplexed single photons and entangled photon pairs from the same source.

## 2. Pulse chirping

To achieve ARP excitation, we require laser pulses of time-varying frequency (chirping). In the frequency domain this is described by

$$E(\omega) = E_0 \exp\left[-\frac{(\omega-\omega_c)^2}{\Delta\omega^2}\right] \exp\left[i\frac{\phi_2}{2}(\omega-\omega_c)^2\right], \tag{1}$$

where $E_0$ is the amplitude of the Gaussian frequency envelope centered at $\omega_c$ with a frequency bandwidth of $\Delta\omega$. The constant $\phi_2$ denotes the group delay dispersion or in general, the linear chirp. In the time domain this pulse again is of Gaussian shape with a time constant $\tau_p$ corresponding to the intensity full width of half maximum (FWHM) and a time varying frequency (while $\tau_0$ is for a transform limited pulse, i.e. $\phi_2 = 0$).

Introducing $\phi_2$ has two effects: it stretches the temporal duration of the laser pulse from $\tau_0$ to $\tau_p$ according to the relation $\tau_p^2 = \tau_0^2 + \left(\frac{4\ln 2(\phi_2)}{\tau_0}\right)^2$, and dictates the frequency ordering in the pulse. For positive $\phi_2$, the frequency increases over time, meaning the red part of the spectrum arrives before the blue part and vice versa for negative $\phi_2$. Additional details on the pulse treatment can be found in SI section appendix A.1.

The experimental implementation of the chirping process is sketched in figure 1(a). Initially, a Ti:Sapphire laser producing pulses of time-width $\tau_0 = 2.7$ ps (measured as intensity autocorrelation FWHM, Tsunami 3950, SpectraPhysics), is tuned to a wavelength of 793 nm.

To render $\phi_2$ we rely on a folded grating stretcher, that consists of a diffraction grating (1200 lines mm$^{-1}$, Newport) to disperse the beam and a lens ($f = 750$ mm) to focus the spectral components to its Fourier plane, where a folding mirror is mounted [53–56]. A motorized slit mounted on the folding mirror enables laser frequency tuning with respect to the two-photon excitation (TPE) resonance. If the distance between the grating and the lens is $f$, laser pulses leave the stretcher dispersion-free, whereas the displacement of the grating towards the lens induces positive chirp [53, 54] (for details see SI). The reason to employ the grating stretcher is that the calculated $\phi_2$ to achieve ARP in our experiment is unachievable with spatial light modulators [40, 42] due to its intrinsic limitations.

Pulse durations corresponding to various grating positions are characterized via spectral and nonlinear autocorrelation measurements (PulseCheck, APE GmbH). The maximum average laser power measured

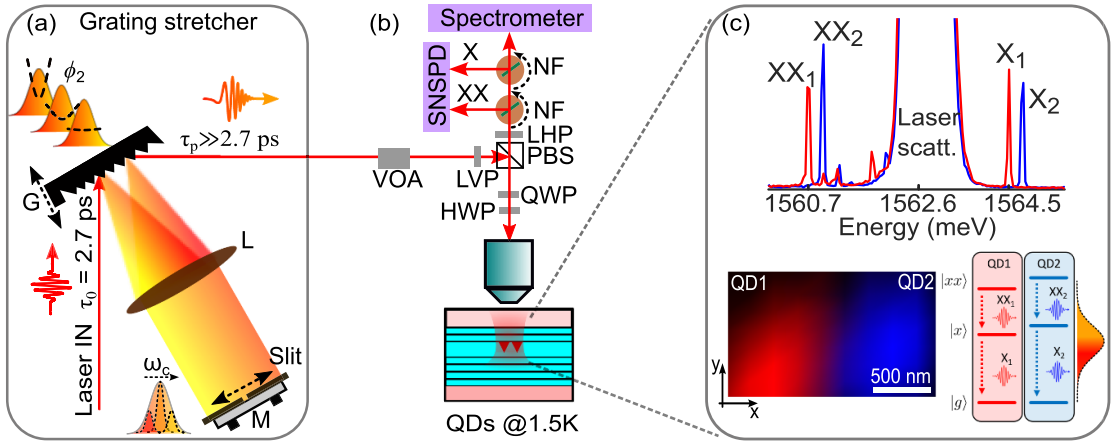


**Figure 1.** Experiment overview: (a) dispersion control: a folded grating stretcher consisting of a ruled grating (G), a lens (L) and a folding mirror (M). A motorized slit mounted on the folding mirror enables laser spectral tuning. The chirp values are varied by translating the grating from the focal plane of the lens. (b) Cryo-microscopy setup: the excitation laser pulses are sent through a variable optical attenuator (VOA) to control pulse power and through polarizing optics (LVP—linear vertical polarizer, PBS—polarizing beamsplitter, HWP—half wave plate, QWP—quarter wave plate) towards an optical cryostat that holds the quantum dot ensemble at 1.5 K. The emitted photons are collected via the same path, cross-polarization filtered with a linear horizontal polarizer (LHP) and sent either towards the spectrometer or through a home-built monochromator equipped with notch filters (NF) to the superconducting nanowire single photon detection (SNSPD) channels to record the exciton (X) and biexciton (XX) photon coincidences. (c) Characterization: the two chosen quantum dots are labelled QD1 and QD2, with their resonant TPE emission spectra, color-coded red (QD1) and blue (QD2) respectively. Also displayed are their raster scan TPE images, alongside a schematic of the involved quantum states.

before the entrance of the stretcher is 400 mW, which corresponds to ≈5 nJ energy per pulse and a peak pulse power of ≈1.8 kW.

## 3. ARP process

The chirped laser pulses exciting the quantum dot induce the ARP process to achieve high-fidelity preparation of the biexciton state. The ARP mechanism relies on a sweep of the instantaneous frequency of the chirped laser pulse across the quantum dot resonance (or electrical Stark tuning under a constant laser pulse [57]). This results in a complete population inversion via an avoided energy level crossing in the dressed state picture [58, 59]. In quantum dots, the ARP mechanism can be applied to excite both the exciton [36, 40, 60] and the biexciton [38, 39, 61] states. Because quantum dots are embedded in a solid-state environment, the interaction with the lattice vibrations (phonons) can cause a deterioration of the ARP process. For low temperatures this process depends on the sign of the chirp [62]. We performed calculations in a standard three-level model consisting of ground $|g\rangle$, exciton $|x\rangle$ and biexciton state $|xx\rangle$ including the exciton-phonon interaction for longitudinal acoustic phonons [39, 63, 64] (for a detailed description see SI). With this, we obtain the biexciton generation for a chirped pulse at $T = 1$ K in figure 2(a), considering a biexciton binding energy of 4 meV. At $\phi_2 = 0$ ps$^2$ we observe Rabi rotations. For $\phi_2 > 0$, we obtain a close to unity biexciton population, quantified by cross-correlation experiments as in [65, 66], for a large range of pulse area and chirp, while for $\phi_2 < 0$, phonons hinder the efficient population of the biexciton.

In the experiments, as shown in figure 1(b), the laser beam coming from the stretcher is fiber-coupled and directed to a closed-cycle cryostat (base temperature 1.5 K, ICEOxford), where the quantum dot sample is mounted on a three-axis piezoelectric stage (ANPx101/ANPz102, attocube systems AG). A programmable electronic variable attenuator (VOA, V800PA, Thorlabs) helps sweeping the pulse power. The setup employs a cross-polarization filtering configuration for efficient laser scattering rejection. The pulse powers are monitored with a 1% reflector (not shown in figure 1(b)) before the polarizing beamsplitter.

The excitation laser beam is focused onto the quantum dots with a cold objective (LT-APO-NIR, NA = 0.81, attocube systems AG). The quantum dot emission is collected via the same path, and the exciton (X) and biexciton (XX) photons are spectrally and spatially separated by a home-built monochromator equipped with four narrow-band notch filters (BNF-805-OD3, FWHM 0.3 nm, Optigrate). The separated

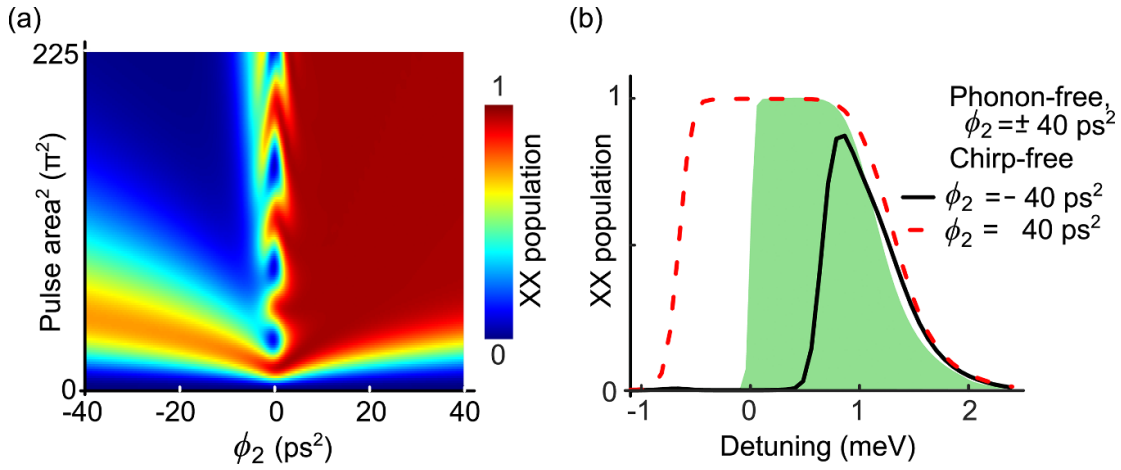


**Figure 2.** Theoretical calculations: (a) biexciton (XX) population under ARP at $T = 1$ K as function of $\phi_2$ and pulse area, starting from a transform limited pulse of $\tau_0 = 2.7$ ps tuned to the TPE resonance. (b) biexciton (XX) population as a function of detuning for chirped excitation ($\phi_2 = \pm 40$ ps$^2$) for pulse area ($\Theta = 20\pi$), $\tau_0 = 2.7$ ps without phonons (blue shaded area) and including phonons at $T = 1$ K (black and red-dashed lines). The green shaded area shows the pure phonon-assisted excitation without chirp at $\tau_0 = 41$ ps and $\Theta = 78\pi$.

photons are routed to a single-photon sensitive spectrometer (Acton SP-2750, Roper Scientific) equipped with a liquid Nitrogen cooled charge-coupled device camera (Spec10 CCD, Princeton Instruments) or superconducting nanowire single-photon detectors (SNSPD, Eos, Single Quantum) for lifetime, cross-correlation and Hanbury Brown-Twiss (HBT) measurements.

## 4. Robustness for simultaneous excitation

The main goal of this work is to excite multiple quantum dots simultaneously. On the single quantum dot level, as evident in figure 2(a), ARP is robust against fluctuations in pulse area and chirp. To excite spectrally distinct quantum dots, we further investigate the efficiency of the biexciton occupation as a function of detuning as shown in figure 2(b) for a chirp of $|\phi_2| = 40$ ps$^2$ and a pulse area of $\Theta = 20\pi$. The detuning $\Delta$ is defined as the difference of the central laser frequency to the TPE resonance, i.e. $\Delta = \hbar(\omega_c - \omega_{TPE})$.

Without phonons (blue area in figure 2(b)), the biexciton occupation does not depend on the sign of $\Delta$. We find that for a detuning range of $-0.45$ meV $\lesssim \Delta \lesssim 0.45$ meV, the biexciton state still gets fully occupied, relying on the ARP process.

If we now include phonons, the behavior of the final occupation changes drastically. For a negative chirp (black curve in figure 2(b)), phonons destroy the ARP process (see also figure 2(a)), and the laser pulses do not lead to any biexciton occupation for a detuning range of $-0.45$ meV $\lesssim \Delta \lesssim 0.45$ meV, while for $\Delta \approx 0.8$ meV, it can get $\approx 80\%$ occupied, due to phonon-assisted processes (for details and an explanation in the dressed states, see SI or [39, 62, 63]).

Most interestingly, for a positive chirp (red-dashed curve in figure 2(b)) the phonons do not hinder the ARP process. Instead, they expand the detuning range suitable for high-fidelity preparation ($\geqslant 95\%$) significantly: $-0.45$ meV $\lesssim \Delta \lesssim 0.75$ meV. We refer to this widening of the detuning window as *phonon advantage*. This implies that the same positively chirped laser pulse can efficiently excite biexciton states in a quantum dot ensemble within a TPE resonance window of $\approx 1.2$ meV.

To underline the effects of the phonon-assisted preparation further, we compare the results to the chirp-free scenario ($\phi_2 = 0$ ps$^2$, shown as green area in figure 2(b)), but with a much higher pulse area of $\Theta \geqslant 78\pi$ and $\tau_0 = 24$ ps (while for the ARP calculation we have used a pulse area of $\Theta = 20\pi$, which corresponds to the same pulse shape after chirping, see SI). For positive detuning $\Delta > 0$, the phonon-assisted process leads to a high biexciton occupation, which agrees with the occupation in the chirped case.

In summary, we observe that for chirped excitation, two different mechanisms lead to the biexciton occupation for positive detuning: the symmetric ARP process (for $|\Delta| \lesssim 0.45$ meV) and the phonon-assisted effect acting at larger positive detunings (0.45 meV $\lesssim \Delta \lesssim 0.75$ meV) (see SI for a detailed discussion).

Given the theoretical background, we now search for a pair of quantum dots, that are spectrally separated within a window of 1 meV. Our sample consists of GaAs-AlGaAs quantum dots with exciton emission centered around 790 nm, grown by the Al-droplet etching method and a surface density of about 0.2 $\mu m^{-2}$ [20, 67].

We locate two bright quantum dots that are spatially separated by $\approx$1 $\mu$m, labeled QD1 (red) and QD2 (blue), (see figure 1(c)). Their characteristic exciton emission lines are found at $X_{QD1} = 792.49$ nm and $X_{QD2} = 792.37$ nm, i.e. they are spectrally separated by 0.12 nm, or 0.2 meV and therefore lie within the window of interest. These quantum dots are not expected to dipole-couple to each other over such a distance. The corresponding TPE spectra, individually measured, are presented in figure 1(c), alongside their representative energy level schemes.

## 5. Individual excitation

We start with the characterization of the two quantum dots QD1 and QD2 (see figure 1(c)) and investigate the robustness of the ARP in comparison to Rabi rotations. To quantitatively illustrate the sensitivity of Rabi rotations to the excitation conditions and quantum dot inhomogeneous broadening, we perform TPE on QD1 and QD2. The excitation- and emission-frequency resolved results are displayed in figures 3(a) and (b). Here, the central laser frequency is scanned in 64 steps from 1562.6 meV to 1563 meV, exploiting the motorized slit in the Fourier plane of the grating stretcher. For every position of the motorized slit, i.e. for a fixed central laser frequency, the TPE Rabi experiment is performed by sweeping the pulse power and recording the emission spectra for QD1 and QD2. Integrating the photon counts at X and XX emission energies illustrates the data in spectrally resolved maps. For brevity, only the photon counts at X emission energy are presented here. Note that in the case of TPE, the laser pulses are tuned to a virtual state that is $\approx$1 meV away from the exciton energy level. Consequently, a direct excitation of the exciton is highly unlikely if not impossible. Therefore, every exciton photon emitted is a consequence of biexciton excitation (the so-called biexciton to exciton to ground state cascaded emission). We also note that the contribution of phonon-assisted TPE is negligible in the explored range of parameters. The linecuts (represented by black dashed lines on the two dimensional maps) denote the respective TPE resonance conditions of QD1 and QD2. The photon counts are normalized to the individual maxima for QD1 and QD2.

For the spectral range 1562.6 meV–1563 meV considered in the experiment, we observe a clear distinction in the X emission landscapes of QD1 and QD2 (figures 3(a) and (b)). For QD1, the resonance frequency is observed at $\approx$1562.64 meV and $\pi$ power is found to be $\approx 5\,\mu$W, while for QD2 the resonance is found at $\approx$1562.88 meV with a $\pi$ power of $\approx 2.5\,\mu$W. In other words, the optimal excitation conditions for QD1 fails to achieve more than 60% population of the biexciton state in QD2 (for example at $\approx$1562.64 meV). This clearly demonstrates the deficiency of Rabi rotation as a universal excitation scheme for multi-quantum dot photon sources.

In figure 3(c) we show the theoretical calculation of the biexciton occupation under TPE. At $\pi$ power, the biexciton population reduces to just $\approx 1.4\%$ when the excitation pulses are blue-detuned by 0.1 meV and to $\approx 0.2\%$ for corresponding red-detuning. Only for high pulse areas $\approx 45\pi$, much beyond the power used in the experiment, would one benefit from the phonon-assisted preparation scheme, that provides a high occupation for the same detuning.

We now turn our attention to the applicability of ARP against spectral shifts in excitation as well as the quantum dot emission. For this we fix $\phi_2 \approx 40$ ps$^2$ and perform the same experiment on QD1 and QD2 (figures 3(d) and (e)). The resulting population landscape is largely a plateau for QD1 and QD2, despite an excitation frequency scan of 0.4 meV, relying on the ARP process. For QD1, the exciton photon counts largely remain stable after 15 $\mu$W onwards, while for QD2, a plateau is reached at 10 $\mu$W, which reflects the differences in their $\pi$ pulse powers. Therefore, despite the energetic separation of QD1 and QD2, ARP can be used to excite the biexciton state with high fidelity within an excitation frequency scan range of 0.4 meV. The robustness of the preparation is again confirmed in the theoretical calculations in figure 3(f) showing an excellent agreement with experiment. It also clearly demonstrates the region of phonon advantage that is asymmetric with respect to the sign of detuning as discussed in figure 2(b). Furthermore, we also investigated the single-photon quality via HBT measurements and obtained the second-order photon correlation of QD2 at Rabi condition as $g^{(2)}(0)_{QD2} = 0.02$ and at ARP regime as $g^{(2)}(0)_{QD2} = 0.05$, respectively, asserting that the single-photon characteristics are maintained at both regimes (see SI).

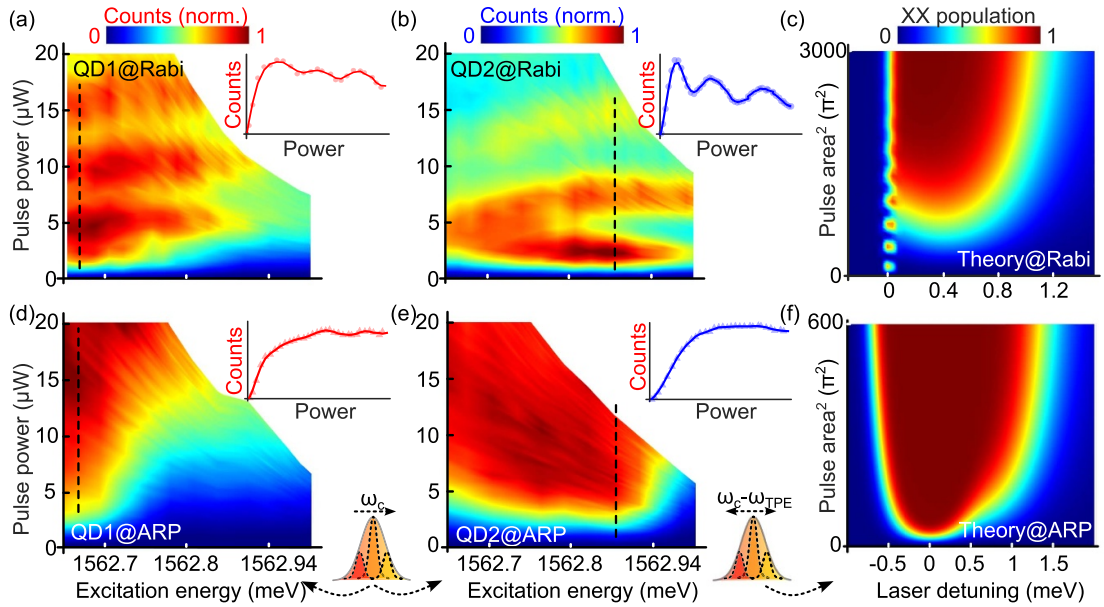


**Figure 3.** Sensitivity of resonant TPE and versatility of ARP: excitation and emission-frequency-resolved TPE Rabi measurements (no chirp, i.e. $\phi_2 = 0$ ps$^2$) represented by measured X photon counts (representative of the XX population) for QD1 (panel (a)) and QD2 (panel (b)). Corresponding results at ARP condition ($\phi_2 = 40$ ps$^2$) for QD1 (panel (d)) and QD2 (panel (e)). The insets show the linecuts at respective TPE resonances (indicated by the black dashed lines on the two-dimensional maps). The integrated photon counts are normalized for QD1 and QD2 individually, but are the same at Rabi ($\phi_2 = 0$ ps$^2$) and ARP ($\phi_2 = 40$ ps$^2$) conditions. (c) Theoretical calculation of the biexciton preparation efficiency under Rabi ($\phi_2 = 0$ ps$^2$) and (f) ARP condition ($\phi_2 = 40$ ps$^2$).

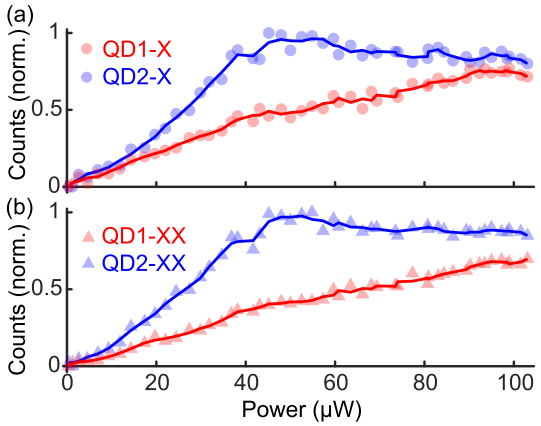


**Figure 4.** Collective excitation at ARP: integrated photon counts at (a) X and (b) XX emission energies for QD1 and QD2 recorded under simultaneous excitation, at $\phi_2 = 40$ ps$^2$ by positioning the excitation laser spot between QD1 and QD2. The photon counts are normalized to a common maximum, respectively for X and XX emissions.

## 6. Simultaneous excitation of two quantum dots

Lastly, we investigated the versatility of ARP to collectively excite QD1 and QD2. For this, we position the objective to simultaneously excite and collect from both QD1 and QD2, resulting in lower photon counts for each. Next we set $\phi_2 \approx 40$ ps$^2$ and keep the frequency spectrum centered at 1562.6 meV. With chirped pulses, we then perform a laser power sweep, recording the collective ARP spectra with a single-mode fiber coupler. In figure 4 we display the integrated photon counts at X and XX emission energies for both quantum dots, normalized to the maximum in either case. We observe that the photon counts of both quantum dots achieve plateaus at high pulse areas (i.e. at ARP regime). This reflects the response we have witnessed earlier in figure 3.

Thus, we have successfully produced two spatially separated quantum dot photon sources that are collectively excited, despite their energetic separation, without modifying the excitation parameters. This is

remarkable; a simple yet elegant excitation scheme where a frequency-chirped laser beam positioned between two spectrally distinct quantum dots, can collectively excite the respective biexciton states with near-unity preparation efficiency. Note that the required pulse power to obtain ARP condition in a simultaneous excitation is much larger than that for individual ARP excitation, because the illuminated area (and hence the average field intensity) is now smaller for either quantum dot individually. That said, the ARP scheme, when applied for simultaneous excitation of multiple dots, does not have a trade-off nor intrinsic limitation to maximize the population, as long as the excitation and the collection is managed efficiently. Compared to the alternative schemes like widefield excitation, our method is simple and is practically free from complex alignment processes and illumination engineering [34]. In such schemes, the photon collection is much more challenging while trying to scale up to more than two quantum dots. Alternatively, in nanowire quantum dots, where individual quantum dots are stacked along the growth direction [68], both the excitation and the collection efficiency restrictions are lifted. Here, one can simultaneously excite ≈20 quantum dots in a confocal excitation volume (which is usually ≈1 $\mu$m for 0.5 numerical aperture). This ensures high-efficiency collective excitation of spectrally distinct, high quality photon sources.

## 7. Conclusions

To conclude, we have presented that simultaneous, high-fidelity preparation of biexciton states is possible in multiple, spectrally distinct quantum dots via chirped laser excitation, relying on ARP. Initially, we showed that near-unity preparation efficiency of biexciton states is maintained in individual quantum dots with resonant energy separation as large as 0.4 meV, clearly establishing the versatility of this scheme against laser frequency fluctuations and quantum dot spectral detunings. Furthermore, we have validated the robustness of the ARP scheme by simultaneously exciting the quantum dots to near-unity biexciton population. These findings support that in future applications two or more entangled photon pairs can be generated using a single excitation pulse, on a suitably-designed quantum dot ensemble in terms of spatial and spectral distribution. We have also presented the theoretical modeling of the scheme based on dressed states, and determined a regime of phonon advantage, wherein the spectral detuning range of quantum dots is widened, and the required pulse power is reduced. Our scheme can be generalized to any quantum dot system and is a significant contribution towards a robust state preparation scheme suitable for enhanced communication rate in quantum dot-based quantum key distribution protocols. In fact, ARP has a wide scope in other research fields too, for instance superresolution imaging, as demonstrated in [69]. In this context, our experiment also provides a significant advancement towards high-resolution, multicolor super resolution imaging [70] using a single laser pulse, being resource-efficient and less bulky.

## Data availability statement

The data that support the findings of this study are available upon reasonable request from the authors. https://doi.org/10.5281/zenodo.7903367.

## Acknowledgments

The authors acknowledge Julian Münzberg, René Schwarz and Daniel Vajner for insightful discussions. F K, Y K, G W and V R acknowledge financial support through the Austrian Science Fund FWF projects W1259 (DK-ALM Atoms, Light, and Molecules), FG 5, TAI-556N (DarkEneT) and I4380 (AEQuDot). T K B and D E R acknowledge financial support from the German Research Foundation DFG through the Project 428026575 (AEQuDot). A R and S F C d S acknowledge C Schimpf for fruitful discussions, the FWF projects FG 5, P 30459, I 4320, the Linz Institute of Technology (LIT) and the European Union's Horizon 2020 research, and innovation program under Grant Agreement Nos. 899814 (Qurope), 871130 (ASCENT+).

## ORCID iDs

Florian Kappe https://orcid.org/0000-0001-6996-8405
Yusuf Karli https://orcid.org/0000-0001-8987-828X
Thomas K Bracht https://orcid.org/0000-0001-7249-6226
Saimon Filipe Covre da Silva https://orcid.org/0000-0003-4977-1933
Tim Seidelmann https://orcid.org/0000-0003-0588-3212
Armando Rastelli https://orcid.org/0000-0002-1343-4962
Gregor Weihs https://orcid.org/0000-0003-2260-3008

Doris E Reiter https://orcid.org/0000-0002-3648-353X
Vikas Remesh https://orcid.org/0000-0003-2029-0570

## References

[1] Uppu R, Midolo L, Zhou X, Carolan J and Lodahl P 2021 *Nat. Nanotechnol.* **16** 1308–17
[2] Zhai L, Nguyen G N, Spinnler C, Ritzmann J, Löbl M C, Wieck A D, Ludwig A, Javadi A and Warburton R J 2022 *Nat. Nanotechnol.* **17** 829–33
[3] Tomm N *et al* 2021 *Nat. Nanotechnol.* **16** 399–403
[4] Liu J 2019 *Nat. Nanotechnol.* **14** 586–93
[5] Senellart P, Solomon G and White A 2017 *Nat. Nanotechnol.* **12** 1026–39
[6] Hanschke L, Fischer K A, Appel S, Lukin D, Wierzbowski J, Sun S, Trivedi R, Vuckovic J, Finley J J and Muller K 2018 *npj Quantum Inf.* **4** 43
[7] Basso Basset F *et al* 2019 *Phys. Rev. Lett.* **123** 160501
[8] Schimpf C, Reindl M, Huber D, Lehner B, Covre Da Silva S F, Manna S, Vyvlecka M, Walther P and Rastelli A 2021 *Sci. Adv.* **7** eabe8905
[9] Jayakumar H, Predojević A, Kauten T, Huber T, Solomon G S and Weihs G 2014 *Nat. Commun.* **5** 4251
[10] Huber T, Ostermann L, Prilmüller M, Solomon G S, Ritsch H, Weihs G and Predojević A 2016 *Phys. Rev.* B **93** 201301
[11] Ding X *et al* 2016 *Phys. Rev. Lett.* **116** 020401
[12] Muller A, Fang W, Lawall J and Solomon G S 2009 *Phys. Rev. Lett.* **103** 217402
[13] Dusanowski Ł, Gustin C, Hughes S, Schneider C and Höfling S 2022 *Nano Lett.* **22** 3562–8
[14] Gustin C, Dusanowski Ł, Höfling S and Hughes S 2022 *Phys. Rev. Res.* **4** 023045
[15] Gerardot B *et al* 2007 *Appl. Phys. Lett.* **90** 041101
[16] Bennett A *et al* 2010 *Nat. Phys.* **6** 947–50
[17] Grim J Q *et al* 2019 *Nat. Mater.* **18** 963–9
[18] Kuklewicz C E, Malein R N, Petroff P M and Gerardot B D 2012 *Nano Lett.* **12** 3761–5
[19] Trotta R, Zallo E, Ortix C, Atkinson P, Plumhof J, Van den Brink J, Rastelli A and Schmidt O 2012 *Phys. Rev. Lett.* **109** 147401
[20] Covre da Silva S F, Undeutsch G, Lehner B, Manna S, Krieger T M, Reindl M, Schimpf C, Trotta R and Rastelli A 2021 *Appl. Phys. Lett.* **119** 120502
[21] Brassard C and Bennett C H 1984 Quantum cryptography: public key distribution and coin tossing *IEEE Int. Conf. on Computers, Systems, and Signal Processing* (https://doi.org/10.1016/j.tcs.2014.05.025)
[22] Kupko T, von Helversen M, Rickert L, Schulze J H, Strittmatter A, Gschrey M, Rodt S, Reitzenstein S and Heindel T 2020 *npj Quantum Inf.* **6** 1–8
[23] Waks E, Inoue K, Santori C, Fattal D, Vuckovic J, Solomon G S and Yamamoto Y 2002 *Nature* **420** 762–762
[24] Heindel T *et al* 2012 *New J. Phys.* **14** 083001
[25] Takemoto K, Nambu Y, Miyazawa T, Sakuma Y, Yamamoto T, Yorozu S and Arakawa Y 2015 *Sci. Rep.* **5** 1–7
[26] Basso Basset F 2021 *Sci. Adv.* **7** eabe6379
[27] Vajner D A, Rickert L, Gao T, Kaymazlar K and Heindel T 2022 *Adv. Quantum Technol.* **5** 2100116
[28] Ramsay A J 2010 *Semicond. Sci. Technol.* **25** 103001
[29] Stufler S, Machnikowski P, Ester P, Bichler M, Axt V M, Kuhn T and Zrenner A 2006 *Phys. Rev.* B **73** 125304
[30] Jayakumar H, Predojević A, Huber T, Kauten T, Solomon G S and Weihs G 2013 *Phys. Rev. Lett.* **110** 135505
[31] Tannor D 2007 *Introduction to Quantum Mechanics* (Mill Valley, CA: University Science Books)
[32] Machnikowski P 2008 *Phys. Rev.* B **78** 195320
[33] Köhler A 1894 *J. R. Microsc. Soc.* **14** 261–2 (available at: https://archive.org/details/zeitschriftfrw10stut/page/36/mode/2up?view=theater)
[34] Heintzmann R and Huser T 2017 *Chem. Rev.* **117** 13890–908
[35] Duquennoy R, Colautti M, Emadi R, Majumder P, Lombardi P and Toninelli C 2022 *Optica* **9** 731
[36] Simon C M *et al* 2011 *Phys. Rev. Lett.* **106** 166801
[37] Wu Y, Piper I M, Ediger M, Brereton P, Schmidgall E R, Eastham P R, Hugues M, Hopkinson M and Phillips R T 2011 *Phys. Rev. Lett.* **106** 067401
[38] Debnath A, Meier C, Chatel B and Amand T 2013 *Phys. Rev.* B **88** 201305
[39] Kaldewey T, Lüker S, Kuhlmann A V, Valentin S R, Ludwig A, Wieck A D, Reiter D E, Kuhn T and Warburton R J 2017 *Phys. Rev.* B **95** 161302(R)
[40] Mathew R, Dilcher E, Gamouras A, Ramachandran A, Yang H Y S, Freisem S, Deppe D and Hall K C 2014 *Phys. Rev.* B **90** 35316
[41] Creatore C, Brierley R T, Phillips R T, Littlewood P B and Eastham P R 2012 *Phys. Rev.* B **86** 155442
[42] Gamouras A, Mathew R, Freisem S, Deppe D G and Hall K C 2013 *Nano Lett.* **13** 4666–70
[43] Ramachandran A, Fraser-Leach J, O'Neal S, Deppe D G and Hall K C 2021 *Opt. Express* **29** 41766
[44] Reiter D, Lüker S, Gawarecki K, Grodecka-Grad A, Machnikowski P, Axt V and Kuhn T 2012 *Acta Phys. Pol.* **122** 1065–8
[45] Ardelt P L *et al* 2014 *Phys. Rev.* B **90** 241404
[46] Bounouar S, Müller M, Barth A M, Glässl M, Axt V M and Michler P 2015 *Phys. Rev.* B **91** 161302
[47] Quilter J, Brash A, Liu F, Glässl M, Barth A, Axt V, Ramsay A, Skolnick M and Fox A 2015 *Phys. Rev. Lett.* **114** 137401
[48] Reindl M, Jöns K D, Huber D, Schimpf C, Huo Y, Zwiller V, Rastelli A and Trotta R 2017 *Nano Lett.* **17** 4090–5
[49] Glässl M, Barth A M and Axt V M 2013 *Phys. Rev. Lett.* **110** 147401
[50] Thomas S E *et al* 2021 *Phys. Rev. Lett.* **126** 233601
[51] Aumann P, Prilmüller M, Kappe F, Ostermann L, Dalacu D, Poole P J, Ritsch H, Lechner W and Weihs G 2022 *AIP Adv.* **12** 055115
[52] Prilmüller M, Huber T, Müller M, Michler P, Weihs G and Predojević A 2018 *Phys. Rev. Lett.* **121** 110503
[53] Backus S, Durfee C G, Murnane M M and Kapteyn H C 1998 *Rev. Sci. Instrum.* **69** 1207–23
[54] Martinez O 1987 *IEEE J. Quantum Electron.* **23** 59–64
[55] Lai M, Lai S T and Swinger C 1994 *Appl. Opt.* **33** 6985
[56] Martinez O E 1986 *J. Opt. Soc. Am.* B **3** 929–34
[57] Mukherjee A, Widhalm A, Siebert D, Krehs S, Sharma N, Thiede A, Reuter D, Förstner J and Zrenner A 2020 *Appl. Phys. Lett.* **116** 251103

[58] Hui H Y and Liu R B 2008 *Phys. Rev.* B **78** 155315
[59] Malinovsky V and Krause J 2001 *Eur. Phys. J.* D **14** 147–55
[60] Wei Y J *et al* 2014 *Nano Lett.* **14** 6515–9
[61] Glässl M, Barth A M, Gawarecki K, Machnikowski P, Croitoru M D, Lüker S, Reiter D E, Kuhn T and Axt V M 2013 *Phys. Rev.* B **87** 085303
[62] Lüker S, Gawarecki K, Reiter D E, Grodecka-Grad A, Axt V M, Machnikowski P and Kuhn T 2012 *Phys. Rev.* B **85** 121302
[63] Lüker S, Kuhn T and Reiter D E 2017 *Phys. Rev.* B **96** 245306
[64] Reiter D E, Kuhn T and Axt V M 2019 *Adv. Phys.* **4** 1655478
[65] Wang H *et al* 2019 *Phys. Rev. Lett.* **122** 113602
[66] Schimpf C, Manna S, Da Silva S F C, Aigner M and Rastelli A 2021 *Adv. Photon.* **3** 065001
[67] Huber D, Reindl M, Huo Y, Huang H, Wildmann J S, Schmidt O G, Rastelli A and Trotta R 2017 *Nat. Commun.* **8** 15506
[68] Laferriere P, Yeung E, Giner L, Haffouz S, Lapointe J, Aers G C, Poole P J, Williams R L and Dalacu D 2020 *Nano Lett.* **20** 3688–93
[69] Kaldewey T, Kuhlmann A V, Valentin S R, Ludwig A, Wieck A D and Warburton R J 2018 *Nat. Photon.* **12** 68–72
[70] Li C, Le V, Wang X, Hao X, Liu X and Kuang C 2021 *Laser Photon. Rev.* **15** 1900084